High-Density Polyethylene/Cycloolefin Copolymer Blends, Part 2: Nonlinear Tensile Creep

Jan Kolařík
Institute of Macromolecular Chemistry, Academy of Sciences of the Czech Republic, 16206 Prague 6, Czech Republic

Alessandro Pegoretti, Luca Fambri, Amabile Penati
Department of Materials Engineering and Industrial Technologies, University of Trento, Trento, Italy

Viscoelastic behavior of most polymeric materials is nonlinear over a major portion of the interval of their response to external forces. The phenomenological theory of viscoelasticity, based on the assumption that molecular (segmental) motions are controlled by available fractional free volume *f*, was found adequate for description of the nonlinear tensile creep, implementation of the time–strain superposition and prediction of the nonlinear creep of studied blends. As *f* of thermoplastics with Poisson's ratio smaller than 0.5 rises proportionally to tensile strain, advancing creep accounts for shortening of retardation times. Consequently, the shift factor along the internal time scale in the time–strain superposition is not constant for a creep curve, but monotonically rises with the elapsed creep time. Compliance curves for various stresses obey fairly well the internal time–strain superposition forming a generalized compliance curve related to an iso-free volume reference state. The predictive format for the blend compliance is based on the parameters characterizing the creep of parent polymers, data on the phase structure of blends obtained from the two-parameter equivalent box model and modified equations of the percolation theory. Applicability of the proposed format is demonstrated on a series of blends of high-density polyethylene with creep-resistant cycloolefin copolymer. POLYM. ENG. SCI., 46: 1363–1373, 2006. © 2006 Society of Plastics Engineers

INTRODUCTION

Resistance to creep is viewed [1–4] as a significant property of polymeric materials whenever end products are exposed to a more or less constant external force (dead load). As generally known, the range of the apparently linear stress–strain relationship of most crystalline thermoplastics does not exceed a few tenths of %. Beyond this limit, the produced strain rises more than linearly with the acting stress [3–9]. There is no doubt that nonlinear viscoelastic behavior predominates over a major portion of the whole response interval of most polymeric materials and plays the key role in most applications. In our previous articles [10–15], we have shown that the stress–strain nonlinearity of thermoplastics observed in the tensile creep can be viewed (at least partly) as a consequence of the strain-induced dilatation [1, 6, 9] that occurs in materials with the Poisson ratio $\nu < 0.5$. After making correction for the strain-induced fractional free volume, we were able to successfully apply the time–strain superposition to compliance curves obtained for a series of stresses [11–15] in the region of nonlinear viscoelasticity.

Creep of thermoplastics can be effectively restrained by admixing a creep-resistant polymer, which forms a co-continuous component. Although creep of many polymers has been described in literature [1–4], much less is known about the creep of polymer blends [16–21]. In our previous articles [11–13] we have studied creep of the polypropylene (PP)/poly(styrene-*co*-acrylonitrile) or PP/cycloolefin copolymer (COC) blends and have proposed a new predictive format for anticipating their nonlinear creep on the basis of experimental data on the creep of constituents. Polyethylene shows a relatively low yield strength and a high propensity to creeping [7]. Thus, search for "reinforcing" yield- and/or creep-resistant components imparting better mechanical properties to PE matrices remains a problem to be solved. In general, attainment of satisfactory mechanical properties of polymer blends frequently depends on finding a suitable compatibilizer, which allows for sufficient interfacial adhesion, finer phase structure, lower tendency to phase structure coarsening, etc. Amorphous ethylene–norbornene copolymers obtained with metallocene-based catalysts [22–24] rank among new polymer materials with remarkable properties, such as a high glass transition temperature (T_g),

transparency, heat resistance, chemical resistance to common solvents, low moisture uptake, high water barrier, and good mechanical properties. The rising percentage of norbornene accounts for an increase in yield or tensile strength and decrease in strain at yielding and break [24] of COC. The latter copolymers are expected [25, 26] to be compatible with PE so that no special compatibilizers are necessary for preparation of the HDPE/COC blends.

In our previous article [27], the phase structure and mechanical properties of the HDPE/COC blends were reported. Of available COC products of Ticona [24] we have used Topas 8007, i.e., the copolymer with the lowest fraction of norbornene (about 30%), which displays yielding and a relatively high strain at break (about 10%). Experimental data for tensile modulus, creep modulus, storage modulus, loss modulus, yield strength, and tensile strength were in good accord with the proposed predictive format based on the equivalent box model (EBM) and modified equations rendered by the percolation theory [28–30]. The applicability of the predictive format was facilitated by the fact that the crystallinity of HDPE is virtually independent of blend composition. In conformity with the percolation concept, mechanical properties revealed the percolation threshold of COC in blends at a lower fraction than microphotographs [27, 31]. The dependencies of yield and tensile strengths on blend composition indicate that interfacial adhesion in the HDPE/COC blends is strong enough to transmit acting stress up to the break point. Strain at break, tensile energy to break and tensile impact strength showed profound drops in the region between 15 and 25% of COC, which corroborated the formation of co-continuous brittle phase of COC.

In this article, we intended to implement a detailed study on creep behavior of the HDPE/COC blends, where the minority COC component imparts better dimensional stability. Our principal objectives were (i) to fit the nonlinear tensile creep of these blends with a suitable equation, (ii) to apply the time–strain superposition involving the strain-induced free volume and (iii) to develop a predictive format appropriate for the creep of binary blends with co-continuous components showing nonlinear creep behavior.

THEORETICAL BACKGROUND OF THE NONLINEAR TENSILE CREEP

Compliance of Thermoplastics

One of the most effective concepts of the phenomenological theory of viscoelasticity [1, 5–9] presumes that the retardation (or relaxation) times are controlled by the free volume available for molecular (segmental) motions. In the case of tensile creep performed under constant temperature and stress, the straining of isotropic solids with Poisson's ratio $v < 0.5$ gives rise to an increment in the free volume owing to their strain-induced expansion. Consequently, the creep behavior becomes nonlinear even at small strains [15],

which makes the analysis of creep data much more complicated. In this section, we will briefly review the format we developed [11–13] to account for the effect of the strain-induced free volume on the nonlinear tensile creep of thermoplastics.

Isothermal tensile compliance $D(t, \sigma)$ of polymers depending on time t and tensile stress σ is customarily viewed as a sum of three components [1, 2]: (i) elastic (reversible) $D_e(\sigma)$; (ii) viscoelastic (reversible) $D_v(t, \sigma)$; (iii) plastic (irreversible) $D_{pl}(t, \sigma)$:

$$D(t, \sigma) = \varepsilon(t,\sigma)/\sigma = D_e(\sigma) + D_v(t,\sigma) + D_{pl}(t,\sigma) \quad (1)$$

where $\varepsilon(t,\sigma)$ is the tensile strain. In this article, we consider the conditions for which $D_{pl}(t,\sigma) = 0$. Creep behavior of polymeric materials is mostly reported in graphical forms [3]. If an experimental creep curve can be fitted with a suitable equation, then storage of data, evaluation of creep rate, interpolation or extrapolation of creep deformation, etc., are facilitated. Several attempts have been made [1, 2, 32–34] to introduce factorization, i.e., to express compliance as a product of independent functions of time or stress. Of numerous empirical functions we have found [11–15] the following equation [35] suitable for the tensile creep of thermoplastics:

$$D(t,\sigma) = W(\sigma)(t/\tau_{rm})^n \quad (2)$$

where $W(\sigma)$ is a function of the stress, τ_{rm} is the mean retardation time and $0 \leq n \leq 1$ is the creep curve shape parameter reflecting the distribution of retardation times.

Effect of the Strain-Induced Free Volume on Tensile Creep of Viscoelastic Solids: The Time–Strain Superposition

The effects of temperature and pressure on viscoelastic behavior of polymers have been successfully interpreted [1, 5–9] in terms of the dimensionless fractional free volume f. Its expansion with increasing (i) temperature (at $T > T_g$) and/or (ii) strain is routinely expressed by the following equation [11–15, 36–38]:

$$f = f_g + \alpha_{fv}(T - T_g) + (1 - 2v)\varepsilon = f_g + \Delta f_T + \Delta f_\varepsilon \quad (3)$$

where f_g is the fractional free volume in the glassy state (customarily viewed [1, 5–9] as an iso-free-volume state) and α_{fv} is the expansion coefficient of the free volume, which can be approximated as the difference between the coefficients above and below T_g, i.e., $\alpha_{fv} = \alpha_1 - \alpha_g$. The available f controls [37–40] retardation (or relaxation) times τ_r of a polymer:

$$ln\ \tau_r = ln\ \Omega + (B/f) \quad (4)$$

where Ω corresponds to the frequency of thermal motion inside a potential well and B is a numerical factor related to the ratio between the volume of a jumping segment and the volume of critical vacancy necessary for a segment jump. The effect of changes in f on a retardation time τ_r is routinely expressed by means of a shift factor along the time scale [1, 5–9, 37–41]. To this end, we have derived [11] the following equation for the time–strain shift factor $log\ a_\varepsilon(\tau_r)$ defined as the ratio of the retardation time $\tau_r(f_2)/\tau_r(f_1)$ at different strains. In terms of the mean retardation time τ_{rm} (at a constant temperature T_c), we consider $\tau_{rm}[\varepsilon(t),T_c]$ at a strain $\varepsilon(t)$ achieved at time t and τ_{rmo} in a selected reference state. If the latter state is identified with the nondeformed state at initial time $t_o = 0$, then $\tau_{rm0}[\varepsilon_0 = 0,T_c]$ is controlled by $f_1=f_g+\alpha_{fv}(T_c-T_g)$:

$$log\ a_\varepsilon(t) = log\ \tau_{rm}(f_2) - log\ \tau_{rm0}(f_1) = -(B/2.303)[(1 - 2v)M\varepsilon(t)/(f_g + \Delta f_{Tc})]/[(1 - 2v)M\varepsilon(t) + (f_g + \Delta f_{Tc})] \quad (5)$$

where $f_2 > f_1$, M is the mean ratio of the actual strain of the most creeping phase in the test specimen and of the measured strain (see below). Combining *Eqs. 2, 5* we obtained [11]

$$log\ D(t,\sigma) = [log\ W(\sigma) - n\ log\tau_{rmi} - n\ log\ a_\varepsilon(t)] + n\ log\ (t) = log\ C(t,\sigma) + n\ log\ t. \quad (6)$$

To separate the effects of time and stress, *Eq. 6* can be rewritten in the form

$$log\ D(t^*,\sigma) = [log\ W(\sigma) - n\ log\tau_{rmi}] + n[log\ t - log\ a_\varepsilon(t)] = log\ C^*(\sigma) + n^*\ log\ t^* \quad (7)$$

where $t^* = t/a_\varepsilon(t)$ denotes the "internal" time of the creep experiment (asterisk is introduced to indicate that the parameters C^* and n^* are related to t^*):

$$log\ t^* = log\ t + (B/2.303)[(1 - 2v)M\varepsilon(t)/(f_g + \Delta f_{T_c})] /[(1 - 2v)M\varepsilon(t) + (f_g + \Delta f_{T_c})]. \quad (8)$$

It should be noted that the time–strain shift factor $log\ a_\varepsilon(t)$ is not constant for an isothermal and isostress creep curve, but grows with the creep strain $\varepsilon(t)$ due to increasing free volume in the creeping specimen. The $log\ D(t)$ vs. $log\ t$ plot would coincide with the corresponding $log\ D(t^*)$ vs. $log\ t^*$ plot for extremely low stresses and strains ($\Delta f_\varepsilon\rightarrow 0$); thus C^* and n^* are the limiting values of C and n for a hypothetical creep in the iso-free volume state corresponding to the initial conditions. Obviously, such dependencies cannot be obtained experimentally because the deformations for $\Delta f_\varepsilon\rightarrow 0$ would be infinitesimally small. *Equation 7* anticipates a linear dependence $log\ D(t^*)$ vs. $log\ t^*$,
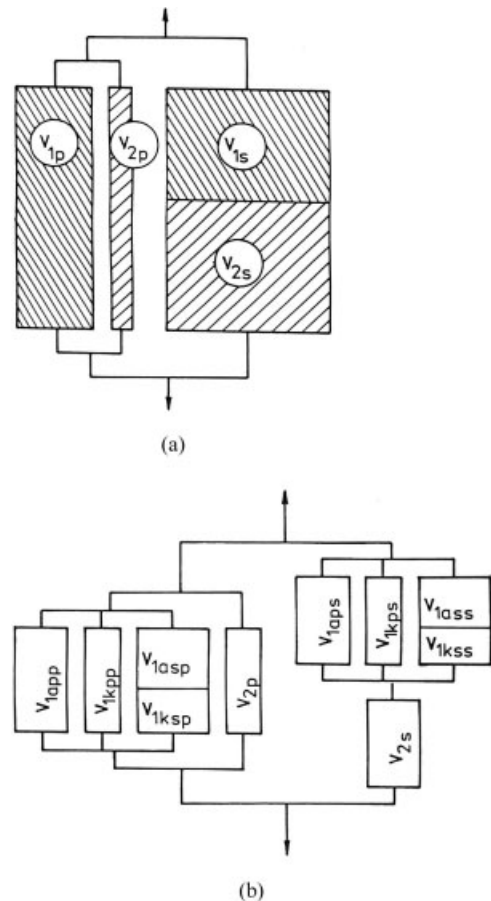

(a)

(b)

FIG. 1. Equivalent box model for a binary blend consisting of (a) two amorphous polymers or (b) a crystalline polymer 1 and an amorphous polymer 2 (schematically).

which, however, has nothing to do with the linear viscoelasticity. Alternatively, to characterize some long-term $log\ D(t^*)$ vs. $log\ t^*$ dependencies, e.g. those of poly(ethylene terephthalate) and of its blends with impact modifiers [14], a polynomial of the second degree was used instead of *Eq. 7*:

$$log\ D(t^*, \sigma) = log\ C_h^*(\sigma) + (a^* + b^*log\ t^*)\ log\ t^*. \quad (9)$$

Compliance of Heterogeneous Binary Blends with Co-continuous Components

Dynamic mechanical and tensile measurements revealed [27] that the HDPE/COC blends with $15 \leq \%\ COC \leq 75$ show partial co-continuity of both components. Binary blends can be modeled [28–30] by means of the EBM given in Fig. 1a, where either component consists of a fraction continuous in the direction of the acting force (v_{1p} or v_{2p}) and of a fraction discontinuous in that direction (v_{1s} or v_{2s}). The resulting compliance of such blends is given as the sum of the contributions of the parallel and series branches:

$$D_b(t) = \{v_{1p}/D_1(t) + v_{2p}/D_2(t) + (v_{1s} + v_{2s})^2/ [D_1(t)v_{1s} + D_2(t)v_{2s}]\}^{-1} \quad (10)$$

where subscripts 1, 2, and b stand for HDPE, COC, and their blends, respectively.

Application of the EBM in the predictive format requires evaluation of the volume fractions v_{1p}, v_{2p}, v_{1s}, and v_{2s}. Utilizing a universal formula for elastic modulus proposed by the percolation theory [42] for binary systems, we have derived [22, 28–30] the following equations for the volume fractions of the EBM:

$$v_{1p} = [(v_1 - v_{1cr})/(1 - v_{1cr})]^q \qquad (11a)$$

$$v_{2p} = [(v_2 - v_{2cr})/(1 - v_{2cr})]^q \qquad (11b)$$

where v_{1cr} and v_{2cr} are the critical volume fractions (the percolation thresholds), at which the respective components become partially continuous, and q is the critical universal exponent. Simpler box models introduced earlier by Takayanagi (detailed information can be found in Ref. 7) differ from our format in two aspects: (i) they do not consider the partial co-continuity of components (phases) typical of polymer blends; (ii) they do not offer any means for a priori evaluation of the input parameters inevitable for the prediction of viscoelastic properties of blends.

By fitting moduli, yield, and tensile strengths as functions of the composition of the HDPE/COC blends, we have found [27] that "universal" values [42–44] $v_{1cr} = 0.156$, $v_{2cr} = 0.156$ and $q = 1.8$ suit well. As the EBM in Fig. 1a is a two-parameter model, only two of the four volume fractions are independent; thus $v_{1s} = v_1 - v_{1p}$ and $v_{2s} = v_2 - v_{2p}$. To describe the compliance of isotropic binary blends with continuous matrix and one dispersed component (such structures occur in the marginal composition ranges), we have modified [10] the Kerner-Nielsen equation [1] for modulus of particulate systems. However, as a first approximation, we can consider the EBM with $v_{1p} = 0$, $v_{1s} = v_1$, for $v_1 < v_{1cr}$ or $v_{2p} = 0$, $v_{2s} = v_2$ for $v_2 < v_{2cr}$.

Strain Magnification Factor of the Creeping Phase in Heterogeneous Blends

As mentioned before, creep of a polymer 1 can be reduced by blending with a polymer 2 having pronouncedly lower compliance (in the temperature range of envisaged applications); however, to achieve this effect, the "reinforcing" component 2 should be partially continuous in the produced blend. If the matrix 1 is crystalline and its T_g is lower than the temperature of creep measurements, then time-dependent molecular motions underlying creep processes in such blends take mainly place in the matrix amorphous phase, which has the highest compliance of the present phases. Thus a binary isotropic blend consisting of a partially continuous crystalline matrix 1 and a partially continuous glassy polymer 2 requires a more complex model [12] (Fig. 1b), where fractions v_{1p} and v_{1s} of the component 1 have to be modeled by means of another ("inserted") EBM. Subscripts of the constituent phases are

TABLE 1. List of the HDPE/COC blends.

HDPE/COC (wt%)	Vol. fract. $(v_1)^a$	Density $(g/cm^3)^b$	X_1 (%)^c	M^d
100/0	1	0.956	68.8	1.82
90/10	0.905	0.960	67.8	1.99
85/15	0.857	0.961	67.7	2.10
80/20	0.809	0.963	65.2	2.19
75/25	0.761	0.969	64.1	2.28
70/30	0.712	0.971	65.2	2.41
60/40	0.614	0.977	62.5	2.57
50/50	0.515	0.981	63.4	2.79
25/75	0.261	0.994	58.6	3.19
0/100	0	1.014	0	—

^{a} Volume fraction of HDPE in blends.
^{b} Data from Ref. 27.
^{c} Crystallinity of as-molded samples in the first DSC scan (data from Ref. 27).
^{d} Strain magnification factor calculated from *Eq. 12*.

1a (amorphous), 1k (crystalline), and 2. In this model, the subscripts of amorphous or crystalline fractions combine letters p and s in various ways according to the hierarchy of couplings in parallel and/or in series.

To account for a relatively higher strain of the amorphous phase, we have introduced [11, 12] the strain-magnifying factor M equal to the mean ratio of the actual (microscopic) strain of the creeping phase 1a and the measured (macroscopic) strain of the creeping specimen. The strain of the fractions v_{1app}, v_{1kpp}, and v_{2p} coupled in parallel (Fig. 1b) is identical with the measured strain. On the other hand, if the component 2 has compliance much lower than the component 1, then the fraction v_{2s} coupled in series is not perceptibly strained. Consequently, the displacement in the fraction v_{1s} is equal to the measured displacement, which means that the resulting strain in the fraction v_{1s} is higher than the measured strain. Following the outlined procedure we have derived [12] the formula for the mean value of M_{1a} of the amorphous phase 1a as the most creeping constituent:

$$M_{1a} = \{v_{1p} - v_{1kpp} + [1 + (v_{2s}/v_{1s})](v_{1s} - v_{1kps})\}/v_{1a} \quad (12)$$

where v_{1a} stands for the volume fraction of the amorphous phase in component 1. Creep-resistant component 2 is assumed to respond to stress as a quasi-elastic material, which means that it mainly affects elastic behavior of blends, while viscoelastic behavior is primarily controlled by component 1. The values of M given in Table 1 were calculated from *Eq. 12* assuming $v_{1cr} = 0.156$ for HDPE and $v_{2cr} = 0.156$ for COC [27]. Similarly, to calculate the fractions v_{1app}, v_{1kpp}, etc. by means of the "inserted" EBM for HDPE, the critical volume fractions were set $\varphi_{1acr} = 0.156$ for amorphous and $\varphi_{1kcr} = 0.156$ for crystalline phases (assuming that $\varphi_{1a} + \varphi_{1k} = 1$). The value of $q = 1.8$ was used in all calculations.

EXPERIMENTAL

Materials

A high-density polyethylene (HDPE), Liten BB 29 (Chemopetrol, Litvínov, Czech Republic) is characterized by melt flow index MFI (230°C, 5 kg) = 1.15 g/10 min (ISO 1133); density (ISO 1183) 0.957 g/cm^3 ; weight–average molar mass M_w = 420,000.

An amorphous COC produced under the trade name Topas 8007 was a product of Ticona, Celanese, Germany, consisting of 30% bicyclo[2.2.1]hept-2-ene (norbornene) units and 70% ethylene units [24]: MFI (230°C, 5 kg) = 34.3 g/10 min; density: 1.014 g/cm^3; T_g = 81°C.

Blend Preparation

A series of HDPE/COC blends was prepared [27] with 10, 15, 20, 25, 30, 40, 50, and 75 wt% of COC (Table 1). Polymers were mixed in the W50EHT mixer of a Brabender Plasti-Corder at 220°C and 60 rpm for 10 min. The initial ratio of the HDPE and COC torques at the processing temperature was about 23/6; a lower relative viscosity of COC was favorable in promoting COC phase co-continuity in blends. Compression molding (press Fontijne; initial temperature: 230°C; pressure 3.1 MPa applied for 2 min; cooling time to room temperature: ca 20 min) was used to obtain plates 120 mm × 100 mm × 1.7 mm from which strips (10 mm in width) for creep measurements were sawn.

Tensile Creep Measurements

Tensile creep was measured by using an apparatus equipped with a mechanical stress amplifier (lever) 10:1. A mechanical strain gauge (with an accuracy of about 2 μm) was connected with the upper clamp of the specimen to indicate the displacement. Specimen dimensions: initial distance between grips 100 mm; cross-section 10 mm × 1.7 mm. Specimens were stored and creep tests were implemented at (23 ± 1)°C. Short-term measurements in the interval 0.1–100 min were performed at five stress levels with one test specimen. Each measurement was followed by a 22 h recovery before another creep test (at a higher stress) was started. Test specimens were used only once for long-term creep measurements in the interval 0.1–10,000 min. Mechanical preconditioning preceding the series of short-term creeps consisted in applying a stress (for 100 min) equal to or higher than the highest stress applied in the series of creep measurements. Long-term measurements were preceded by application of a stress, which produced within 100 min a strain larger than the expected final strain of the intended experiment; the following recovery (before the recorded creep was initiated) was about 24 h. Specimens for creep studies were stored for more than 6 months at room temperature to exclude a possible interfering effect of physical aging during creep measurements.

RESULTS AND DISCUSSION

The Time–Tensile Strain Superposition of Compliance Dependencies for Different Stresses

The stress–strain linearity is evidenced by coinciding compliance curves obtained at different stresses. Figure 2a including five short-term creeps of HDPE shows that the increasing stress accounts for (i) an increase in $D(t,\sigma)$ and (ii) an increase in the creep rate defined as the derivative $d \log D(t,\sigma)/d \log(t)$. Obviously, the as-measured compliance curves for different stresses cannot be superposed by means of simple shifts along the given axes. The proposed alternative procedure consists in plotting $\log D(t,\sigma)$ against the logarithm of "internal" time t^*. However, this approach is hampered by a series of problems associated with availability, reliability and accuracy of the input data, i.e., B, f_g, α_{fv}, M, and ν. The value of B is generally believed, with regard to its definition, to be a constant close to 1. However, lower or higher values of B were reported, namely $0.5 < B < 1$ [45] or $2.3 < B < 3.2$ [46]. The fractional free volume in the glassy state f_g = 0.025 is regarded as an average universal constant. However, T_g of HDPE was reported [1] between 153 and 233 K; thus, T_g = 193 K may be a reasonable value [47]. The coefficient of the free volume thermal expansion $\alpha_{fv} = \alpha_1 - \alpha_g = 3.9 \ 10^{-4} \ K^{-1}$ is given in Ref. 48. Employing these values we obtain $(f_g + \Delta f_{T_c})$ = $0.025 + 3.9 \ 10^{-4}K^{-1}(296 \ K - 193 \ K) \cong 0.065$. Although the size of free volume vacancies in PE [49, 50] and COC [51] has recently been studied by positron annihilation lifetime spectroscopy, no data on $(f_g + \Delta f_{T_c})$ have been reported.

Similar problems are related to Poisson's ratio of thermoplastics and to its possible dependencies on time and/or strain presumed by the theory [1, 49, 52, 53]. However, only constant values of ν are usually tabulated to characterize polymers [1, 2, 48]. Although Poisson's ratio is indispensable for comprehensive description of mechanical properties of polymeric materials, sporadic data occurring in the literature are often uncertain due to questionable methods of measurement. Epoxies and rubber-modified epoxies showed a virtually linear increase in the volume with tensile strain in the region of reversible deformation [54], which indicates a constant ν. In creep experiments, polycarbonate [55], poly(methyl methacrylate) [55] and plasticized epoxies [56] exhibited a small increase in ν with tensile deformation. Tensile creep of poly(vinyl chloride) indicated the rise in $v(\varepsilon,t)$ with time and applied stress in the interval $0.39 < v(\varepsilon,t) < 0.45$ [52]. Available literature [48, 57] reports ν = 0.42 for HDPE.

Figure 2b shows that the compliance curves for different stresses do not superpose, if B = 1, $(f_g + \Delta f_{T_c})$ = 0.065, v = 0.42 and M = 1.82 (Table 1) are used in *Eq. 8*. However, the superposition could be reached through reasonable adjustments of some inputs. The criteria for the selection of a modified set of the inputs can be defined as follows: (i) selected inputs are acceptable from the physical
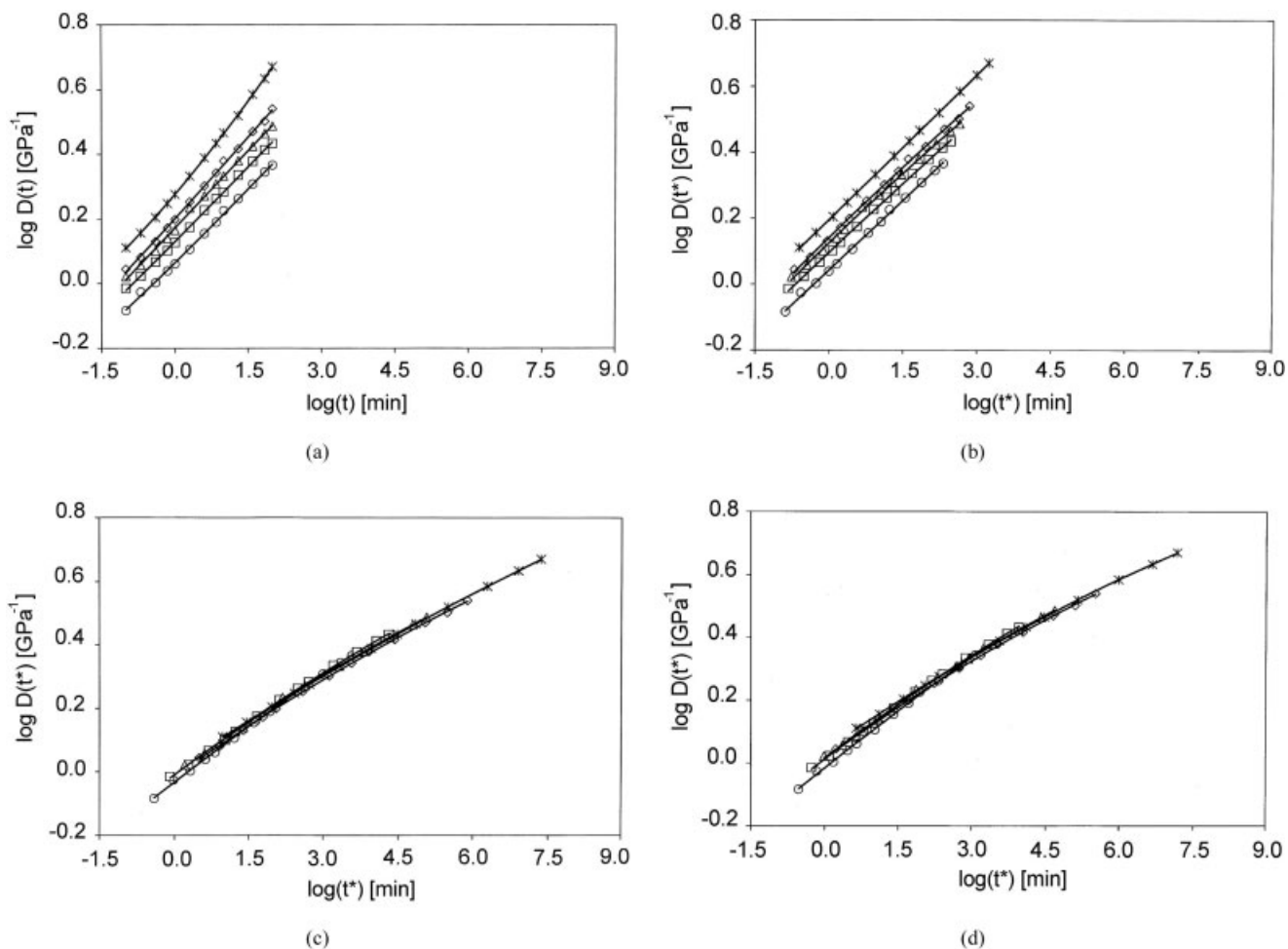
FIG. 2. Superposition of the short-term tensile creep dependencies of HDPE. Applied stress (in MPa): (o) 4.63; ($\square$) 6.17; ($\triangle$) 7.72; ($\diamond$) 9.26; (x) 10.81. Inputs: $\nu = 0.42$; $M = 1.82$. (a) data plotted against real time log t; (b) data plotted against internal time log t^* calculated for $B = 1$, $(f_g + \Delta f_{T_c}) = 0.0652$; (c) data plotted against internal time log t^* calculated for $B = 1$, $(f_g + \Delta f_{T_c}) = 0.028$ (the average parameters calculated from the values read off for five short-term compliance dependencies are given in Table 2); (d) data plotted against internal time log t^* calculated for $B = 4.2$, $(f_g + \Delta f_{T_c}) = 0.0652$.

point of view; (ii) short-term compliance dependencies obtained for five different stresses superpose to form a smooth generalized dependence in the $log\ D(t^*)$ vs. $log\ t^*$ coordinates; (iii) this generalized dependency coincides with an experimentally determined long-term dependency. It is evident that $B = 1$ or $(f_g + \Delta f_{T_c}) = 0.065$ is relatively more uncertain than $\nu = 0.42$ and $M = 1.82$. It can be shown that an increase in M or a decrease in ν leads to a mere extension of the internal time scale. On the other hand, a decrease in $(f_g + \Delta f_{T_c})$ or an increase in B also accounts for expansion of the time scale, but if either of these quantities exceeds a certain "critical" value, then the sequence (along the $log\ D$ axis) of superposed curves is inverted. Thus it is obvious that a plausible superposition can be attained via adjustments of $(f_g + \Delta f_{T_c})$ and/or B. Empirically, we have found that five short-term curves superpose quite well for $(f_g + \Delta f_{T_c}) = 0.028$ and unmodified $B = 1$ (Fig. 2c). An equivalent generalized dependence can be obtained for $B = 4.2$ and unmodified $(f_g + \Delta f_{T_c}) = 0.065$ (Fig. 2d). However,

the latter combination may seem less realistic so that we use the former data set for superposition of compliance dependencies and for evaluation of the parameters in Eqs. 7 and 9 (Table 2). Moreover, Fig. 2c and 2d reveal an important fact that even though the superposition is attained with different series of inputs, the shape of the generalized curve and its position on the internal time scale are virtually identical. This finding implies that it is not possible to arbitrarily fix the generalized curve on the time scale by manipulating with the inputs, because a successful superposition can be attained only in a certain interval on the t^* scale ("reference state"), which was also documented for PP in our previous article [15].

Creep behavior of COC at 23°C has been reported in our previous article [13]. In brief, it contrasts with that of HDPE (Table 2) because the compliance of COC is much lower and almost independent of time. Therefore, the parameters in Eqs. 7 and 9 are much smaller than those found for HDPE. However, relatively high stresses (applied to pro-

TABLE 2. Effect of stress on the parameters in *Eqs. 7* and *9*.

Test	Stress[a]	log C*	n*	R[2][b]	log C$_h$*	a*	b*	R$_h$[2][b]
HDPE								
STC[c]	7.72	0.0038	0.0986	0.9982	−0.0154	0.1127	−0.0026	0.9996
e.s.d.[d]	—	0.0232	0.0100	—	0.0098	0.0073	0.0006	—
GenCrv[e]	—	0.0050	0.0956	0.9908	−0.0175	0.1180	−0.0036	0.9970
LTC[f]	5.37	0.0147	0.0896	0.9844	−0.0271	0.1342	−0.0065	0.9995
HDPE/COC = 90/10								
STC	9.12	−0.0653	0.0946	0.9976	−0.0822	0.1115	−0.0023	0.9996
e.s.d.	—	0.0155	0.0079	—	0.0123	0.0095	0.0027	—
GenCrv	—	−0.0617	0.0915	0.9924	−0.0855	0.1133	−0.0034	0.9978
LTC	5.94	−0.0810	0.0910	0.9905	−0.1133	0.1250	−0.0050	0.9995
HDPE/COC = 85/15								
STC	10.37	−0.0714	0.0818	0.9982	−0.0864	0.1014	−0.0022	0.9996
e.s.d.	—	0.0078	0.0054	—	0.0119	0.0101	0.0012	—
GenCrv	—	−0.0609	0.0839	0.9874	−0.0802	0.0980	−0.0019	0.9900
LTC	6.31	−0.0631	0.0818	0.9894	−0.0965	0.1138	−0.0046	0.9988
HDPE/COC = 80/20								
STC	10.43	−0.0671	0.0860	0.9988	−0.0773	0.0939	−0.0007	0.9995
e.s.d.	—	0.0064	0.0044	—	0.0088	0.0071	0.0007	—
GenCrv	—	−0.0623	0.0838	0.9961	−0.0757	0.0927	−0.0011	0.9971
LTC	7.00	−0.0595	0.0750	0.9879	−0.0994	0.1090	−0.0045	0.9991
HDPE/COC = 75/25								
STC	12,47	−0.1275	0.0825	0.9995	−0.1334	0.0878	−0.0009	0.9998
e.s.d.	—	0.0082	0.0038	—	0.1008	0.0076	0.0008	—
GenCrv	—	−0.1240	0.0808	0.9982	−0.1336	0.0867	−0.0007	0.9986
LTC	8.29	−0.0928	0.0746	0.9926	−0.1349	0.1017	−0.0003	0.9993
HDPE/COC = 70/30								
STC	12.69	−0.1441	0.0777	0.9993	−0.1486	0.0823	−0.0008	0.9998
e.s.d.	—	0.0069	0.2734	—	0.0057	0.0077	0.0009	—
GenCrv	—	−0.1384	0.0757	0.9969	−0.1457	0.0803	−0.0006	0.9972
LTC	8.19	−0.1335	0.0694	0.9919	−0.1654	0.0949	−0.0034	0.9991
HDPE/COC = 60/40								
STC	12.92	−0.2168	0.0705	0.9989	−0.2140	0.0712	−0.0004	0.9997
e.s.d.	—	0.0118	0.0028	—	0.0213	0.0103	0.0016	—
GenCrv	—	−0.2239	0.0727	0.9969	−0.2204	0.0700	−0.0004	0.9970
LTC	10.76	−0.1833	0.0556	0.9937	−0.2184	0.0782	−0.0026	0.9997
HDPE/COC = 50/50								
STC	13.56	−0.2435	0.0556	0.9992	−0.2481	0.0602	−0.0009	0.9997
e.s.d.	—	0.0085	0.0019	—	0.0096	0.0051	0.0007	—
GenCrv	—	−0.2451	0.0558	0.9970	−0.2506	0.0605	−0.0007	0.9975
LTC	16.05	−0.2297	0.0522	0.9987	−0.2475	0.0607	−0.0008	0.9997
HDPE/COC = 25/75								
STC	19.72	−0.3683	0.0249	0.9951	−0.3620	0.0209	0.0000	0.9979
e.s.d.	—	0.0223	0.0034	—	0.0344	0.0086	0.0012	—
GenCrv	—	−0.3989	0.0229	0.8307	−0.4057	0.0363	-0.0012	0.8330
LTC	21.13	−0.3544	0.0261	0.9515	−0.2992	−0.0013	0.0028	0.9793
COC								
STC	18.57	−0.5670	0.0068	0.9641	0.2038	0.0041	0.0003	0.9908
e.s.d.	—	0.0152	0.0006	—	0.0061	0.0012	0.0004	—
GenCrv	—	−0.4700	0.0103	0.3816	−0.4662	0.0052	0.0013	0.3877
LTC	15.68	−0.5103	0.0151	0.9556	−0.4985	0.0026	0.0022	0.9921

[a] Tensile stress in MPa.
[b] Reliability coefficients.
[c] Short-term creep (100 min)—mean value of tensile stress for five measurements
[d] Estimated standard deviation.
[e] Parameters of the generalized compliance curve obtained by fitting the data of five STC.
[f] Long-term creep (more than 10,000 min).

duce measurable strains) account for a small decrease in the elastic part of the compliance. For this reason, the generalized curve ($B = 1$, $f_g + \Delta f_{T_c} = 0.025$, $v = 0.35$, $M = 1$) fitting the data of five 100 min measurements is characterized by lower values of the reliability parameters (Table 2).

To reduce the number of figures, experimental results are only reported for the HDPE/COC 50/50 blend, which shows
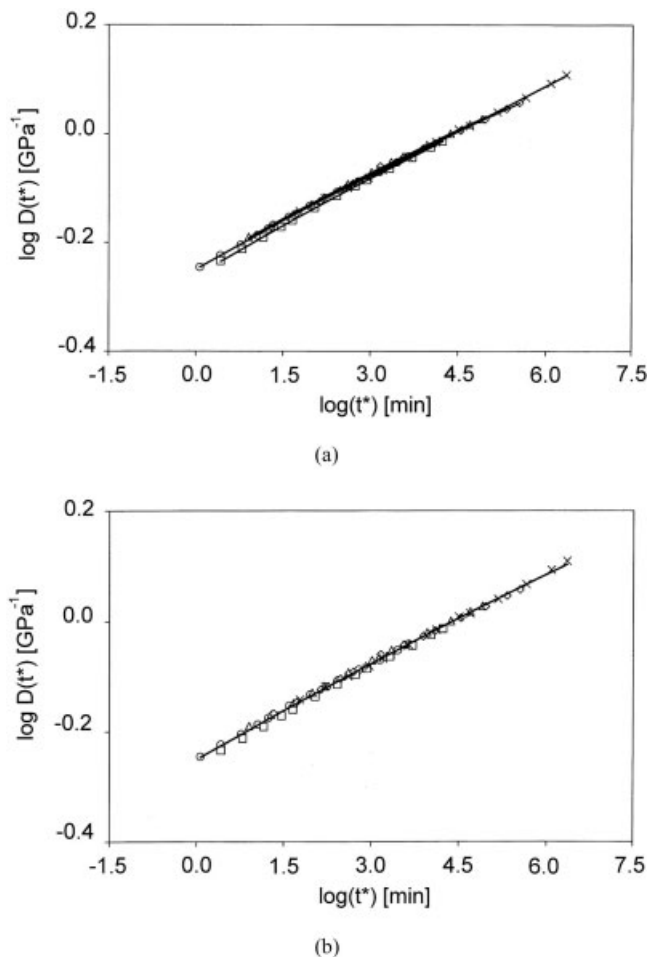
(a)

(b)

FIG. 3. Superposition of the short-term tensile creep dependencies of the HDPE/COC = 50/50 blend. Applied stress (in MPa): (o) 8.14; (□) 10.85; (△) 13.57; (◇) 16.28; (x) 19.00. Data plotted against internal time log t^* using $B = 1$, $(f_g + \Delta f_{T_c}) = 0.028$, $\nu = 0.42$, $M = 2.79$. (a) data for each stress approximated by a polynomial of the second degree; (b) all data approximated by one polynomial of the second degree (cf. Table 2).

a much lower compliance than HDPE because of the reinforcing effect of COC forming a co-continuous phase as documented in Ref. 27. If the strain-induced free volume is taken into account, five short-term dependencies $log\ D_b(t^*)$ vs. $log\ t^*$ superpose (Fig. 3a) with the aid of the same inputs used for HDPE in Fig. 2c. All the plotted experimental data are fairly well approximated by one generalized curve in Fig. 3b. Thus, Figs. 2 and 3 concurrently show that the compliance dependencies determined in the region of nonlinear viscoelasticity can be superposed over the whole measured time intervals if they are reconstructed for a constant (initial) free volume. In this way, the nonlinear creep behavior becomes apparently linear in the co-ordinates $log\ D(t^*, \sigma)$ vs. $log\ t^*$, which is in conformity with our previous articles [12–15].

Creep data of all prepared HDPE/COC blends are summarized in Table 2, which reveals a decrease in compliance with rising fraction of COC in blends. In parallel, the parameters n^*, a^*, and b^* characterizing the effect of time become smaller. The differences between R_h (data fitting by
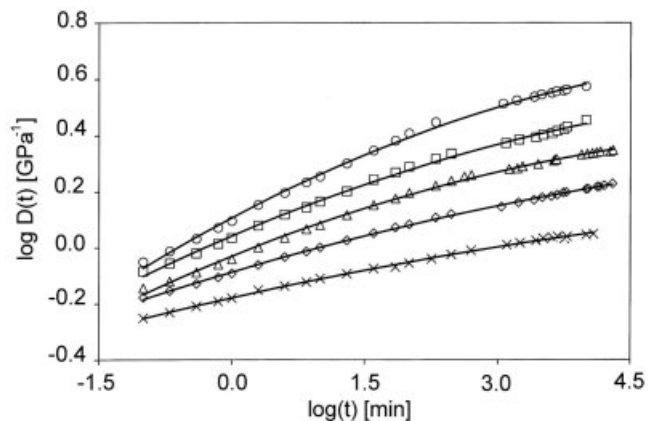

FIG. 4. The $log\ D(t)$ vs. log t dependencies for long-term tensile creep of the HDPE/COC blends. Composition of blends (Table 1) and applied stress (in MPa): (o) 100/0, 5.46; (□) 80/20, 7.00; (△) 70/30, 8.19; (◇) 60/40, 10.76; (x) 50/50, 10.88.

Eq. 9) and *R* (data fitting by *Eq. 7*) diminish because the shape of the $log\ D(t^*)$ vs. $log\ t^*$ curves approaches straight lines due to decreasing b^*. Nevertheless, the values of R_h consistently remain somewhat higher than corresponding values of *R*. Although *Eq. 9* permits better fitting of experimental data, e.s.d. (estimated standard deviation) for a^* and particularly for b^* are higher than e.s.d. for n^* of *Eq. 7*, which can be attributed to the fact that *Eq. 9* is more sensitive to possible irregularities in individual dependencies, e.g. to the read-off displacements shortly after the load imposition.
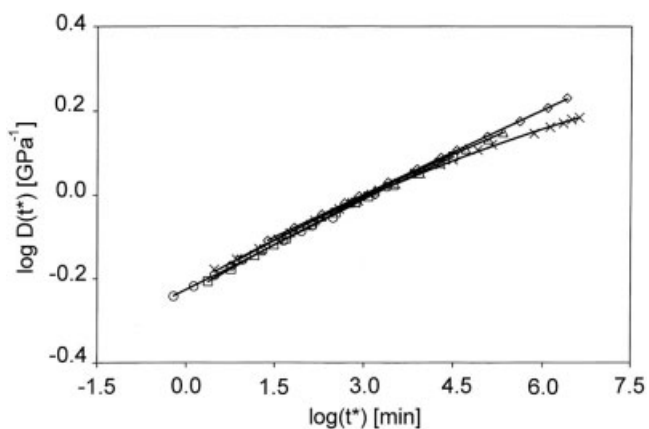
Comparison of Superposed and Long-Term Compliance Dependencies

Long-term creeps of HDPE and of the blends containing 20, 30, 40, or 50% of COC plotted against real time are compared in Fig. 4. Owing to the nonlinear viscoelastic behavior of the HDPE/COC blends, these plots are somewhat affected by differences in $\varepsilon(t,\sigma)$ and related Δf_ε produced in the course of creep measurement of materials showing different stiffness. As can be seen, the shape of plots reflects the effect of $b^* < 0$ of the HDPE matrix. The rising fraction of COC decreases the compliance of blends and the negative value of b^* (cf. Table 2). A slight decrease in the creep rate $d\ log\ D(t,\sigma)/d\ log(t)$ at long creep periods is an inherent property of the used HDPE, which might be attributed to a type of deformation stiffening. It is worth noting that PP [13, 15] showed $b^* \cong 0$, while poly(ethylene terephthalate) [14] displayed $b^* > 0$.

Figure 5 compares four short-term $log\ D(t^*)$ vs. $log\ t^*$ dependencies at elevated stresses with a corresponding long-term dependency at a lower stress. The short-term curves of the 75/25 blend coincide quite well with the long-term curve, which slightly deviates towards lower compliance with rising creep time (Fig. 5a). Quite analogous patterns can be observed also for the 60/40 blend (Fig.
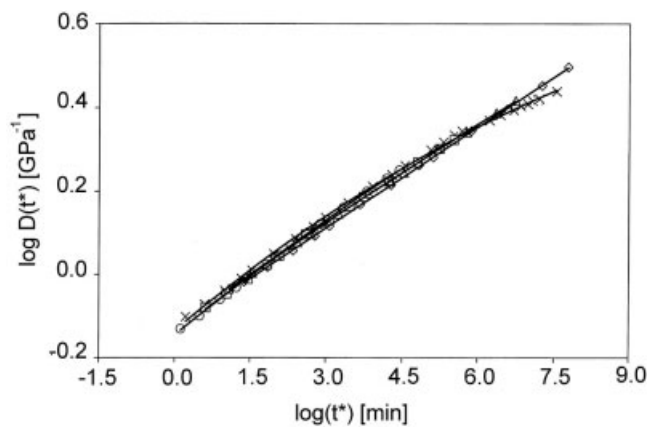
(a)

(b)

FIG. 5. Comparison of four superposed short-term creeps (STC) with long-term creep curve (LTC). Data are plotted against internal time $log\ t^*$ calculated for $B = 1$, $(f_g + \Delta f_{Tc}) = 0.028$ and $\nu = 0.42$; values M are given in Table 1. Data for each creep are approximated by one line. Composition of blends (Table 1) and applied stress (in MPa): (a) HDPE/COC = 75/25: STC: (o) 8.06; (□) 10.75; (△) 12.90; (◇) 14.51; LTC: (x) 8.29. (b) HDPE/COC = 60/40: STC: (o) 6.35; (□) 10.59; (△) 13.24; (◇) 15.89; LTC: (x) 10.76.

5b). Negative b^* of the HDPE matrix obviously does not manifest itself in the series of short-term experiments, because it is not sufficiently pronounced at creep times shorter than 100 min. For this reason, the parameters in *Eqs. 7, 9* extracted from the superposed short-term creeps are somewhat more "pessimistic" than the parameters from the long-term curves (Table 2). Nonetheless, the parameters in *Eqs. 7, 9* read off for the superposed dependencies (consisting of five 100 min measurements) and experimental long-term dependencies are in a reasonably good accord for all the tested blends (Table 2), which indicates that a series of short-term creeps can effectively substitute long-term measurement.

Prediction of the Time-Dependent Compliance of Blends in the Nonlinear Stress–Strain Region

The predictive format for the blend compliance requires experimentally ascertained parameters in *Eq. 7* or *9* for
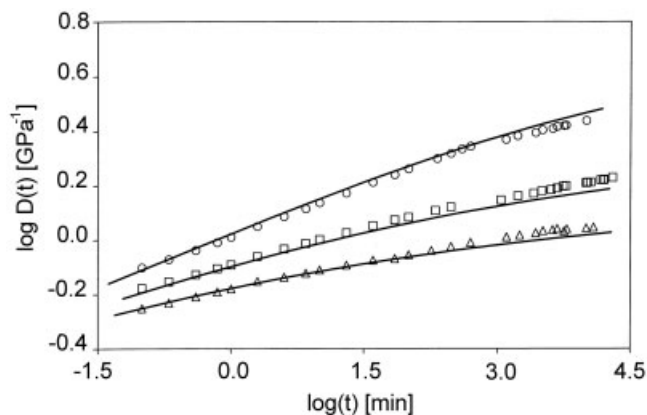

FIG. 6. Comparison of long-term experimental (data points) and predicted compliance curves (full lines) for selected HDPE/COC blends. Blend composition (weight %) and applied stress (MPa): (o) HDPE/COC = 75/25; 8.29; (□) 60/40; 10.76; (△) 50/50; 10.88. Inputs for HDPE: $C_{1h}^* = 0.9605$ GPa^{-1}; $a_1^* = 0.118$; $b_1^* = -0.0036$; inputs for COC: $C_2^* = 0.271$ GPa^{-1}; $n_2^* = 0.0068$; inputs for blends: $B = 1$; $(f_g + \Delta f_{Tc}) = 0.028$; $\nu = 0.42$; M, Table 1.

HDPE and COC. Introducing these data into *Eq. 10*, we obtain

$$log\ D_b(t^*) = log\ \{[(v_{1p}/C_1^*t^{*y}) + (v_{2p}/C_2^*t^{*z})$$
$$+\ v_s^2/(v_{1s}C_1^*t^{*y} + v_{2s}C_2^*t^{*z})]^{-1}\} \quad (13)$$

where $v_s = v_{1s} + v_{2s}$, $y = n_1^*$ or $(a_1^* + b_1^*\ log\ t^*)$ and $z = n_2^*$ or $(a_2^* + b_2^*\ log\ t^*)$. With regard to the differences in creep behavior of the components we will use $log\ D_1(t^*) = log\ C_{1h}^* + (a_1^* + b_1^*\ log\ t^*)\ log\ t^*$ and $log\ D_2(t^*) = log\ C_2^* + n_2^*\ log\ t^*$.

The calculated $log\ D(t^*)$ vs. $log\ t^*$ dependency for a material can be transformed into the real $log\ D(t)$ vs. $log\ t$ dependency for any selected stress lower than the yield strength. The corresponding real time t is obtained by introducing $\varepsilon(t) = \sigma D(t)$ into *Eq. 5*:

$$log\ a_\varepsilon = -(B/2.303)[(1-2v)M\sigma D(t)/(f_g + \Delta f_{Tc})]$$
$$/[(1-2v)M\sigma D(t) + (f_g + \Delta f_{Tc})] \quad (14)$$

$$As\ log\ t = log\ t^* + log\ a_\varepsilon, \quad (15)$$

a series of data points obtained by using *Eq. 13* can be plotted against log t.

Experimental and calculated long-term compliance curves of the 75/25, 60/40, and 50/50 blends are compared in Fig. 6. The given values of C^*, a^*, and b^* used in *Eq. 14* were extracted from the short-term creeps (Table 2); the remaining inputs were identical with those used in the superposition procedure. The compliance curves calculated for the blends fit experimental data point quite well over the entire studied time interval. Comparison of Figs. 4 and 6 indicates that the discussed uncertainties in the input data do not preclude a fairly good prediction of compliance curves

if the input parameters are identical with those used in the internal time–strain superposition.

CONCLUSIONS

Creep resistance of the HDPE/COC blends is proportional to the COC fraction. HDPE and HDPE-rich blends show highly nonlinear creep behavior because increasing stress accounts for (i) an increase in $D(t,\sigma)$ and (ii) an increase in the creep rate defined as the derivative $d\,log\,D(t,\sigma)/d\,log(t)$. Thus, the as-measured compliance curves for different stresses cannot be superposed by simple shifts along the given axes. The phenomenological theory of viscoelasticity, based on the assumption that molecular (segmental) motions are controlled by available fractional free volume f, was found adequate for the description of nonlinear tensile creep, implementation of the time–strain superposition and the prediction of nonlinear creep for any tensile stress lower than yield strength. The internal time t^* was introduced to account for a continuous shortening of retardation times caused by available f rising in proportion to the creep strain, which occurs in materials with Poisson's ratio smaller than 0.5. Consequently, the shift factor along the time scale in the time–strain superposition is not constant for a creep curve, but monotonically increases from point to point with the elapsed creep time. The $log\,D(t^*)$ vs. $log\,t^*$ dependencies obtained for various stresses fairly well obey the time–strain superposition thus forming a generalized creep curve (over extended time scale) related to an iso-free volume reference state. Credibility of generalized curves (constructed by using several short-term creep tests at elevated stresses) was proved by their comparison with experimental long-term curves.

The predictive format for the time-dependent compliance $D_b(t^*)$ of the HDPE/COC blends requires as the input data (1) the parameters characterizing the creep of parent polymers and (2) data on the phase structure of blends. The latter problem was solved by using (i) the two-parameter EBM and (ii) calculations of the phase continuity parameters for the components based on modified equations of the percolation theory. The predicted long-term compliance dependencies of blends are in fairly good conformity with experimental data.

ACKNOWLEDGMENTS

REFERENCES

1. L.E. Nielsen and R.F. Landel, *Mechanical Properties of Polymers and Composites*, Marcel Dekker, New York (1994).

2. R.J. Crawford, *Plastics Engineering*, Butterworth Heinemann, Oxford (1998).

3. W. Andrew, *The Effect of Creep and Other Time Related Factors on Plastics and Elastomers*, Plastics Design Library, New York (1991).

4. W.N. Findley, J.S. Lai, and K. Onaran, *Creep and Relaxation of Nonlinear Viscoelastic Materials*, North-Holland, Amsterdam (1976).

5. J.J. Aklonis, W.J. MacKnight, and M. Shen, *Introduction to Polymer Viscoelasticity*, Wiley-Interscience, New York (1972).

6. J.D. Ferry, *Viscoelastic Properties of Polymers*, Wiley, New York (1980).

7. I.M. Ward and D.W. Hadley, *An Introduction to the Mechanical Properties of Solid Polymers*, Wiley, Chichester (1993).

8. F. Rodriguez, *Principles of Polymer Systems*, Taylor & Francis, Washington, DC (1996).

9. E. Riande, R. Diaz-Calleja, M.G. Prolongo, R.M. Masegosa, and C. Salom, *Polymer Viscoelasticity*, Marcel Dekker, New York (2000).

10. J. Kolařík, L. Fambri, A. Pegoretti, A. Penati, and P. Goberti, *Polym. Eng. Sci.*, **42**, 161 (2002).

11. J. Kolařík, *J. Polym. Sci. B: Polym. Phys.*, **41**, 736 (2003).

12. J. Kolařík, A. Pegoretti, L. Fambri, and A. Penati, *J. Appl. Polym. Sci.*, **88**, 641 (2003).

13. J. Kolařík, A. Pegoretti, L. Fambri, and A. Penati, *Macromol. Mater. Eng.*, **288**, 629 (2003).

14. A. Pegoretti, J. Kolařík, G. Gottardi, and A. Penati, *Polym. Int.*, **53**, 984 (2004).

15. J. Kolařík and A. Pegoretti, *Polymer*, **47**, 346 (2006).

16. C.B. Bucknall, *Toughened Plastics*, Applied Science, London (1977).

17. L.A. Utracki, *Polymer Alloys and Blends*, Hanser, Munich (1990).

18. M.J. Folkes and P.S. Hope, *Polymer Blends and Alloys*, Chapman & Hall, Cambridge (1993).

19. L.H. Sperling, *Polymeric Multicomponent Materials*, Wiley, New York (1997).

20. L.A. Utracki, *Commercial Polymer Blends*, Chapman & Hall, London (1988).

21. D.R. Paul and C.B. Bucknall, editors, *Polymer Blends*, Wiley, New York (1999).

22. L. Tritto, L. Boggioni, J.C. Jansen, K. Thorshaug, M.C. Sacchi, and D.R. Ferro, *Macromolecules*, **235**, 616 (2002).

23. K. Thorshaug, R. Mendichi, L. Boggioni, I. Tritto, S. Trinkle, C. Friedrich, and R. Muelhaupt, *Macromolecules*, **35**, 2903 (2002).

24. Topas COC, brochure from Ticona, Hoechst, Germany (1995).

25. D. Rana, C.H. Lee, K. Cho, B.H. Lee, and S. Choe, *J. Appl. Polym. Sci.*, **69**, 2441 (1998).

26. J. Luettmer-Strathmann and J.E.G. Lipson, *Macromolecules*, **32**, 1093 (1999).

27. J. Kolařík, Z. Kruliš, M. Šlouf, and L. Fambri, *Polym. Eng. Sci.*, **45**, 817 (2005).

28. J. Kolařík, *Eur. Polym. J.*, **34**, 585 (1998).

29. J. Kolařík, A. Pegoretti, L. Fambri, and A. Penati, *J. Polym. Res.*, **7**, 1 (2000).

30. J. Kolařík, L. Fambri, A. Pegoretti, and A. Penati, *Polym. Eng. Sci.*, **40**, 127 (2000).

31. M. Šlouf, J. Kolařík, and L. Fambri, *J. Appl. Polym. Sci.*, **91**, 253 (2004).

32. M. Schlimmer, *Rheol. Acta*, **18**, 62 (1979).

33. F.Y.C. Boey, T.H. Lee, and K.A. Khor, *Polym. Test.*, **14**, 425 (1995).

34. J.X. Li and W.L. Cheung, *J. Appl. Polym. Sci.*, **56**, 881 (1995).

35. R.W. Garbella, J. Wachter, and J.H. Wendorff, *Prog. Colloid Polym. Sci.*, **71**, 164 (1985).

36. J.D. Ferry and R.A. Stratton, *Kolloid-Z.*, **171**, 107 (1960).

37. W.G. Knauss and I. Emri, *Polym. Eng. Sci.*, **27**, 86 (1987).

38. G.U. Losi and W.G. Knauss, *Polym. Eng. Sci.*, **32**, 542 (1992).

39. N.G. McCrum, B.E. Read, and G. Williams, *Anelastic and Dielectric Effects in Polymeric Solids*, Wiley, London (1967).

40. W.G. Knauss and I.J. Emri, *Comput. Struct.*, **13**, 123 (1981).

41. R.A. Schapery, *Polym. Eng. Sci.*, **9**, 295 (1969).

42. P.G. De Gennes, *J. Phys. Lett. (Paris)*, **37**, L1 (1976).

43. W.Y. Hsu and S. Wu, *Polym. Eng. Sci.*, **33**, 293 (1993).

44. J. Sax and J.M. Ottino, *Polym. Eng. Sci.*, **23**, 165 (1983).

45. K. Ito, Y. Saito, T. Yamamoto, Y. Ujihira, and K. Nomura, *Macromolecules*, **34**, 6153 (2001).

46. C.F. Popelar and K.M. Liechti, *J. Eng. Mater. Technol.*, **119**, 205 (1997).

47. P.C. Painter and M.M. Coleman, *Fundamentals of Polymer Science*, Technomic, Lancaster, PA (1997).

48. D.W. Van Krevelen, *Properties of Polymers*, Elsevier, Amsterdam (1997).

49. M. Misheva, N. Djourelov, A. Dimitrova, and G. Zamfirova, *Macromol. Chem. Phys.*, **201**, 2348 (2000).

50. J. Borek and W. Osoba, *Polymer*, **42**, 2901 (2001).

51. G. Zamfirova, M. Misheva, E. Perez, R. Bonavente, M.L. Cerrada, N. Djourelov, M. Kresteva, and J.M. Perena, *Polym. J.*, **34**, 779 (2002).

52. R.S. Lakes, *Viscoelastic Solids*, CRC, Boca Raton (1999).

53. N.W. Tschoegl, W.G. Knauss, and I. Emri, *Mech. Time-Dependent Mater.*, **6**, 3 (2002).

54. Z.H. Stachurski, *Prog. Polym. Sci.*, **22**, 407 (1997).

55. H. Bertilson, M. Delin, J. Kubat, W.R. Rychwalski, and M. Kubat, *J. Rheol. Acta*, **32**, 361 (1993).

56. P.S. Theocaris, *Polymer*, **20**, 1149 (1979).

57. N.E. Dowling, *Mechanical Behavior of Materials*, Prentice Hall, Upper Saddle River, NJ (1999).